Numerical modeling of spray cooling-assisted dermatologic laser surgery for treatment of port wine stains

Walfre Franco[a,b], Rong Zhang[b], J. Stuart Nelson[b], and Guillermo Aguilar[a,b]

[a]Dept. of Mechanical Engineering, University of California, Riverside, CA 92521
[b]Beckman Laser Institute Medical Clinic, University of California, Irvine, CA 92612

ABSTRACT

Cryogen spray cooling (CSC) provides thermal protection to the epidermis during dermatologic laser surgery (DLS) for removal of port wine stain (PWS) birthmarks. The objectives of this paper are: to improve the thermal modeling of skin undergoing CSC-assisted DLS for PWS treatment; and, to address the effect of temporal and lateral variations in surface heat transfer during CSC on epidermal protection. The finite element method is used to solve the two-dimensional light and heat diffusion equations in a skin-cross section composed by epidermis, dermis and two blood vessels. Thermal conductivities of each biological structure are modeled as temperature dependent functions. The model accounts for the latent heat of fusion and vaporization, and temporal and spatial thermal variations—due to the inherent non-homogeneous nature of sprays—in surface cooling. Thermal damage due to laser irradiation is evaluated by an Arrhenius integral model. For a 60 ms cryogen spurt, temperature maps of epidermis show that at the end of the spurt there are significant temperature differences, which resulted in epidermal damage after a 5 J/cm^2 0.45 ms laser pulse at 585 nm on light color skin type. A 60 ms delay between end of spurt and laser onset produced a relative more homogeneous temperature distribution at the epidermis, and, subsequently, a more effective CSC-DLS for which only the blood vessels were thermally damaged. Temporal and lateral variations in surface cooling must be taken into account to guarantee that enough epidermal protection is provided. Thermal and optical numerical models of CSC-assisted DLS procedures that incorporate all the complexity of the problem are a valuable and fundamental research tool.

Keywords: Spray cooling, dermatologic laser surgery, thermal damage

1. NOMENCLATURE

A	frequency factor (1/s)
C	specific heat (J/kg/K)
c	speed of light in i (m/s)
D	optical diffusion coefficient (m)
E_a	activation energy barrier (J/mole)
F	laser fluence (J/m^2)
f_l	laser frequency (1/s)
f_∞	surrounding light frequency (1/s)
g	optical anisotropy factor
h	heat transfer coefficient (W/m^2/K)
I_l	laser output irradiance (W/m^2)
I_∞	surrounding light irradiance (W/m^2)
k	thermal conductivity (W/m/K)
p	Planck's constant (J·s)
Q_f	water's latent heat of fusion (J/kg)
Q_v	water's latent heat of vaporization (J/kg)
q_c	spray cooling heat flux (W/m^2)
R	universal gas constant (J/mole/K)
r	reflection factor

Send correspondence to wfranco@ucr.edu, gaguilar@ucr.edu

T	temperature (K)
T_u	core-body blood temperature (K)
T_∞	surrounding temperature (K)
t	time (s)
t_p	laser pulse duration (s)
t_c	spray cooling duration (s)
u	mass of blood per volume unit per time unit (kg/m^3/s)
V	correction factor
x	lateral coordinate (m)
y	depth coordinate (m)

Greek letters

μ_a	linear absorption coefficient (1/m)
μ_s	linear scattering coefficient (1/m)
μ_{tr}	transport attenuation coefficient (1/m)
ρ	density (kg/m^3)
ϕ	photon fluence (number of photons/m^2/s)
Ω	thermal damage

Superscripts

b	blood
d	dermis
e	epidermis
i	biological structure (epidermis, dermis, blood)
v	vacuum

2. INTRODUCTION

Light irradiation at specific wavelengths is commonly used in dermatologic laser surgery (DLS) to treat vascular superficial lesions and abnormalities, such as port wine stains (PWS) birthmarks. The task of DLS is to induce irreversible thermal damage to undesired structures embedded within the dermis. Cryogen spray cooling (CSC) controls unintended heating at the epidermis—because of melanin absorption—by lowering selectively the temperature of epidermis prior to laser irradiation.[1] CSC has significantly improved the effectiveness of DLS and become an integral part of it by providing epidermal protection, allowing application of higher laser fluences, easing patient discomfort and permitting to treat patients with higher contents of melanin.[2] Although CSC-assisted DLS has proved to be quite effective, there are still important limitations on the procedure and lack of knowledge about the physics of spray, laser and tissue interactions.

The therapeutic outcome of CSC-assisted DLS depends, among many biological and non-biological factors, on the choice of parameters within spray and laser systems. Numerical modeling is an efficient way—sometimes the only one—to evaluate these parameters by predicting clinical outcomes. Therefore, there is a need to continue developing and integrating mathematical models of light transport, heat transfer and thermal damage on biological structures. Several significant numerical studies about CSC and DLS have been carried out by different authors. Most of these studies are about DLS, and those including CSC are usually restricted to the center of the laser beam axis or assume uniform boundary conditions at the skin surface. However, experimental studies on skin phantoms[3] and aluminum surfaces[4] have shown that there is only uniform cooling within a small radius ($\approx$ 2 mm), and that temperature differences between the center and perimeter of the sprayed surface may be as large as 20 °C.[5] In this study, we simulate CSC-assisted DLS of PWS on a skin cross-section to address the effect of lateral variations in cooling on epidermal protection.

We use diffusion theory to approximate the photon distribution within tissue. This approximation is appropriate if scattering rather than absorption dominates in the medium, and if the radiance is only slightly anisotropic. Close to the boundary, where light enters the tissue, radiation is highly anisotropic and, thus, corrections must be applied. This is also true for sources.

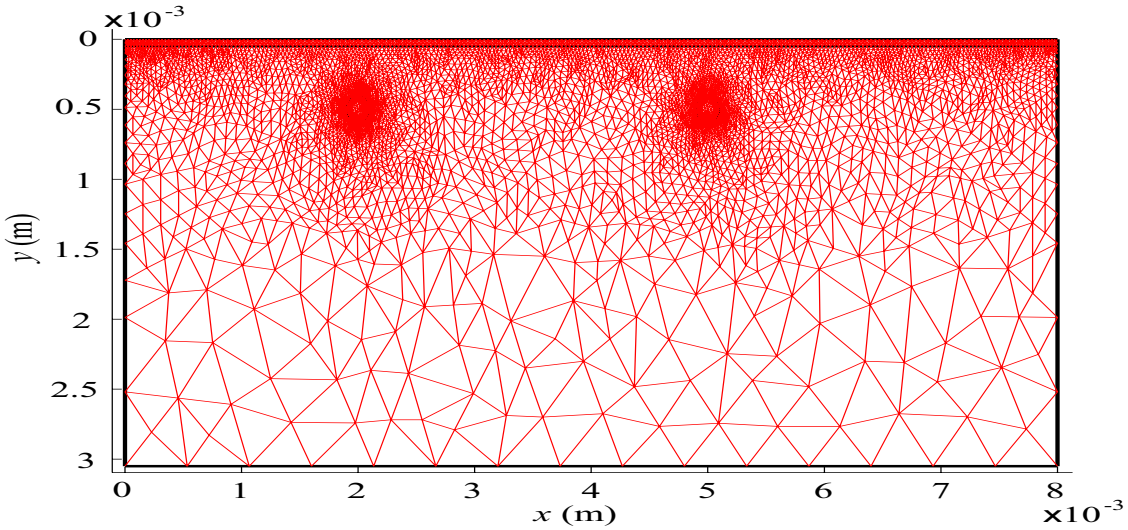

Figure 1. Skin cross-section geometry and FEM mesh.

To calculate temperature fields we use the bioheat transfer equation with a light absorption heat source and without the metabolic heat source because it has a negligible influence on the thermal field compared to that of the temperature gradients imposed by cryogen spray cooling and laser irradiation. To improve the thermal simulation we model thermal conductivities of epidermis, dermis and blood as temperature-dependent functions, for which published correlations for specific temperature ranges are used. Since it is not easy to measure thermal and optical properties within tissue, there are many gaps and uncertainties on reported values. To fill some of these gaps we interpolate and make basic assumptions. The model also accounts for the latent heat of fusion and evaporation of water in the heat capacity. Finally, to evaluate thermal damage of tissue we use a—first order kinetic or Arrhenius—rate process analysis.

3. MATHEMATICAL MODELS

The light and heat diffusion equations are solved using the finite element method (FEM) within a commercial software (Femlab, Comsol Inc., Burlington MA). Figure 1 shows the skin geometry and FEM mesh: epidermis (50 μm thick) on top of two blood vessels (each with 100 μm radius) embedded within dermis (8×3 mm). The center of the first vessel is 2 mm away from the laser beam axis ($x = 0$) and 500 μm deep (i.e., $x = 2 \times 10^{-3}$ and $y = 0.5 \times 10^{-3}$), and the center of the second vessel is at the same depth but 5 mm away from the axis (i.e., $x = 5 \times 10^{-3}$ and $y = 0.5 \times 10^{-3}$). The radii of the sprayed and radiated surfaces are 8 and 6 mm, respectively.

3.1. Light Transport

The light diffusion equation—which follows from Fick's and conservation of energy laws[6–8]—without a source term is

$$\frac{\partial}{\partial t}\phi_i(x,y,t) - c_i\nabla\left(D_i\nabla\phi_i(x,y,t)\right) = -c_i\mu_{a,i}\phi_i(x,y,t), \tag{1}$$

where t is the time, ϕ_i is the photon fluence rate, x and y are the lateral and depth coordinates respectively, c_i is the speed of light, and $\mu_{a,i}$ is the linear absorption coefficient. The optical diffusion coefficient $D_i = 1/(3\mu_{tr,i})$, and the transport attenuation coefficient $\mu_{tr,i} = \mu_{a,i} + (1-g)\mu_{s,i}$, where $\mu_{s,i}$ is the linear scattering coefficient and g_i is the optical anisotropy factor. The subscript $i = e$, d and b denotes epidermis, dermis and blood, respectively. Equation 1 implies that the rate of change of energy density at a specific location is equal to the energy diffused away minus the energy absorbed at that location. Laser light is modeled as a flux of photons at the top boundary as

$$\frac{(1-r)I_l c_o}{pf_l} = -D_e c_e \nabla\phi_e(x,y,t), \tag{2}$$

for $0 \leq x \leq 8 \times 10^{-3}$ and $y = 0$. $r = 0.1$ is the reflection factor, c_v is the speed of light in vacuum (3×10^8 m/s), p is Planck's constant (6.63×10^{-34} J·s), and f_l is the laser frequency. The laser output irradiance per time unit I_l is defined as the ratio between laser fluence F and pulse duration t_p.[9] At the bottom and right edges of the skin cross section the boundary condition is

$$-D_d \nabla \phi_d(x, y, t) = \phi_d(x, y, t), \tag{3}$$

for $x = 8 \times 10^{-3}$, $0 \leq y \leq 3 \times 10^{-3}$; and $0 \leq x \leq 3 \times 10^{-3}$, $y = 3 \times 10^{-3}$. Because of symmetry,

$$\nabla \phi(x, y, t) = 0, \tag{4}$$

at the laser beam axis, $x = 0$, and $0 \leq y \leq 3 \times 10^{-3}$. The initial distribution of the optical field is

$$\phi_i(x, y, 0) = \frac{I_\infty}{p f_\infty} \exp(-\mu_{a,i}\, y), \tag{5}$$

where I_∞ and f_∞ are the irradiance and frequency of surrounding light—I_∞ does not affect the skin temperature.

3.2. Heat Transfer

The heat transfer equation in tissue can be expressed as

$$\rho_i C_i \frac{\partial}{\partial t} T_i(x, y, t) - \nabla(k_i \nabla T_i(x, y, t)) = \rho_i C_i u (T_u - T_i(x, y, t)) + \mu_{a,i} \phi_i(x, y, t) p f_l V_i, \tag{6}$$

where ρ_i is the density, C_i is the specific heat, T_i is the temperature, k_i is the thermal conductivity, u is the mass of blood per cubic meter per second, T_u is the blood (core-body) temperature of unaffected vessels, and V_i is the correction factor for ϕ at the epidermis and blood vessels. Values of V_e (0.37) and V_b (0.47) are determined by comparison to a Monte Carlo solution. The first term on the right hand side of Eq. 6 accounts for the effect of blood perfusion, and the second term accounts for the photon absorption of chromophores in tissue. In the epidermis, we use a melanosome absorption coefficient of 40000 1/m at 585 nm[10] and a melanin volume fraction of 5%— light skin type; in the blood, we assume 0.4 hematocrit content for the blood vessels. The initial temperatures of epidermis, dermis and blood are 300, 310 and 310 K (27, 37 and 37 °C), respectively.

At the skin surface, the thermal boundary condition is

$$-k \nabla T_i(x, y, t) = \begin{cases} q_c(y, t) & \text{if } t \leq t_c, \\ h(T - T_\infty) & \text{if } t > t_c, \end{cases} \tag{7}$$

for $0 \leq x \leq 8 \times 10^{-3}$ and $y = 0$. During cooling, $t \leq t_c$, a space and time dependent heat flux $q_c(y, t)$ extracts heat from the skin. q_c was calculated using temperature measurements from previous experiments of CSC on skin phantoms and an analytical expression based on Duhamel's theorem and Fourier's law—measurements and analytical methodology can be found in the literature[11]—under the assumption that similar temperature dynamics can be imposed on human skin. During laser irradiation and afterward, $t > t_c$, air flows over the skin surface, hence the free convection boundary condition is modeled using the heat transfer coefficient $h = 150$ W/K/m^2 of air flowing over a hot plate.[12] At the other tissue boundaries

$$\nabla T(x, y, t) = 0, \tag{8}$$

for $x = 8 \times 10^{-3}$, $0 \leq y \leq 3 \times 10^{-3}$; $0 \leq x \leq 3 \times 10^{-3}$, $y = 3 \times 10^{-3}$; and, $x = 0$, $0 \leq y \leq 3 \times 10^{-3}$.

The specific heat is modeled as

$$C_i = C_i + Q_{v,i} \frac{\exp\left(-\frac{(T_i - 373)^2}{\Delta T_i^2}\right)}{\sqrt{\pi \Delta T_i^2}} + Q_{f,i} \frac{\exp\left(-\frac{(T_i - 273)^2}{\Delta T_i^2}\right)}{\sqrt{\pi \Delta T_i^2}}, \tag{9}$$

where $Q_{v,i}$ and $Q_{f,i}$ are the water's latent heat of vaporization and fusion, respectively. Phase transitions are assumed to occur over $\Delta T = 1$ K. The thermal conductivity as a function of temperature is modeled as

$$k_i^j = \begin{cases} b_i^j / T_i^{m_i^j} & (T \text{ in K}) \quad \text{if } T < 276 \text{ K}, \\ m_i^j T_i + b_i^j & (T \text{ in } ^\circ\text{C}) \quad \text{if } 270 \leq T \leq 276 \text{ K}, \\ m_i^j T_i + b_i^j & (T \text{ in } ^\circ\text{C}) \quad \text{if } T > 276 \text{ K}. \end{cases} \tag{10}$$

The values of m_i and b_i for each range of temperatures are given in Table 1. Based on the high water content of epidermis and dermis, we use k of ice in the subzero region ($T < 270$ K) as the conductivities of epidermis and dermis.[13] k_b in this region is a fit of clinical data.[13] In the region above zero ($T > 276$ K), k_e and k_d models are based on Valvano et al.[14] linear regression on several tissues at different temperatures; in this study, the linear model was shifted so that k_e and k_i coincide with reported values at room conditions.[15] k_b in this region is calculated using Singh and Blackshear's model.[15, 16] In the region of phase transition ($270 \leq T \leq 276$) we assume a linear dependence on temperature for k_e, k_d and k_b.

range	j	m_e	b_e	m_d	b_d	m_b	b_b
$T < 276$	1	1.235	2135	1.235	2135	1005	1.15
$270 \leq T \leq 276$	2	0.6342	-0.1557	0.8804	-0.1311	0.7844	-0.0872
$T > 276$	3	0.1632	0.001265	0.4832	0.001265	0.5159	0.00226

Table 1. constants

3.3. Thermal Damage

We use a rate process analysis of thermal damage Ω_i to calculate the epidermal damage and hemoglobin coagulation as

$$\Omega_i = A_i \int_0^t \exp\left(-\frac{E_{a,i}}{R\,T_i(x,y,\tau)}\right) d\tau, \tag{11}$$

where A_i is the frequency factor, $E_{a,i}$ the activation energy threshold and R the universal time constant (8.32 J/mole/K). Values of skin and blood coefficients are shown in Table 2.

	A (1/s)	E_a (J/mole)
Bulk skin[17]	3.1×10^{98}	628,000
Hemoglobin[18]	7.6×10^{66}	455,000

Table 2. Thermal Damage Process Coefficients

	epidermis	dermis	blood
μ_a (1/m)	2000	24	19100
μ_s (1/m)	47000	12,900	46700
n	1.37	1.37	1.33
g	0.79	0.79	0.995
ρ (kg/m^3)	1200	1200	1100
C (J/kg K)	3600	3800	3600
Q_f (J/kg)	1800×10^3	1575×10^3	1350×10^3
Q_e (J/kg)	267×10^3	234×10^3	200×10^3

Table 3. Optical and Thermal Properties

Coagulation profiles are calculated by assuming that the coagulation threshold for irreversible damage occurs when 63% of tissue is damaged,[19] i.e. $\Omega_i = 1$. Table 3 shows optical and thermal properties of epidermis, dermis

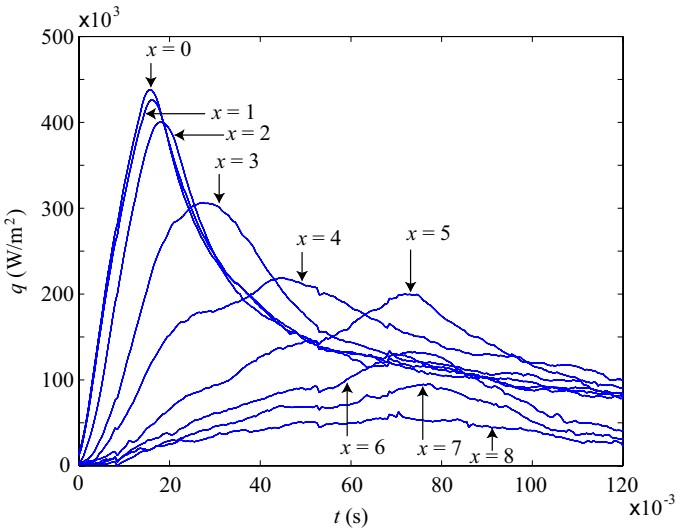

Figure 2. Cooling boundary condition.

and blood. Optical properties correspond to 585 nm wavelength. Q_e, Q_d and Q_b correspond to 80%, 70% and 60% of the evaporation ($2,250 \times 10^3$ J/kg at 100 °C) and fusion (334×10^3 J/kg at 0 °C) latent heat of water.[20]

In this study, two different CSC-DLS sequences are modeled: the first one, simulates a 60 ms liquid cryogen spurt and a 0.45 ms laser pulse; the second one is similar to the first one plus a 60 ms delay between the end of the spurt and laser onset. The spray and laser beam radii are 8 and 6 mm, respectively, and the laser wavelength and fluence are 585 nm and 5 J/cm^2, respectively.

4. RESULTS AND DISCUSSION

Figure 2 shows $q_c(x,t)$ which is obtained by using surface temperature data from Franco et al.[11] and an analytical approximation for direct calculation of surface heat flux.[11,21] This figure shows the thermal boundary condition during cooling, q_c, as a function of time every 1 mm along the 8 mm radius of the sprayed surface; cooling conditions correspond to a 60 ms cryogen spurt, the spray cone has an 8 mm radius at the surface and its central axis is at $x = 0$. Note that there are considerable differences between central ($x = 0, 1, 2$) and peripheral ($x = 6, 7, 8$) locations, in general, the closer the location is to the center: the higher the maximum q_c is; the earlier q_c maximum rises; and, the more marked the dynamic variation of q_c is. Therefore, epidermal protection provided during CSC is non-uniform laterally and temporally.

Isothermal contours in °C within epidermis are shown in Fig. 3 at two different times during the first CSC-DLS sequence: at the end of the 60 ms cryogen spurt, Fig. 3(a), and after a 0.45 ms laser pulse, Fig. 3(b). There is no delay between CSC and laser irradiation. The initial temperature of epidermis is 27 °C and because of the non-uniform heat extraction, as expected, there are significant temperature variations within the epidermal layer at the laser onset in Fig. 3(a): the lowest isothermal contour is 2 °C with a lateral range and depth of ≈ 5 mm and 20 μm, respectively; the highest isothermal contour is 27 °C, that is, there is an epidermal region underneath the sprayed surface that has not been cooled at all. Figure 3(b) shows that at the end of laser exposure, the highest isothermal contours at 67 °C are located approximately at a 20–45 μm depth within a 5.5 mm radius; for a point at $x = 0$ and $y = 35$ μm, $\Omega_e = 5$. Therefore, regardless of photocoagulation success of the targeted blood vessels, this CSC-DLS sequence is not viable. Temperature gradients along the lateral coordinate x are mainly due to the non-homogenous nature of sprays, for which average impact velocity and size of droplets and liquid to vapor ratio decrease from the spray axis to the periphery—this is even more remarkable in evaporation liquids, such as cryogenic sprays. Temperature gradients along the depth coordinate y are due to the thermal-insulation nature of epidermis, which is slow for conveying heat by conduction and requires a great deal of energy for temperature changes—i.e., thermal conductivity is low and specific heat is high.

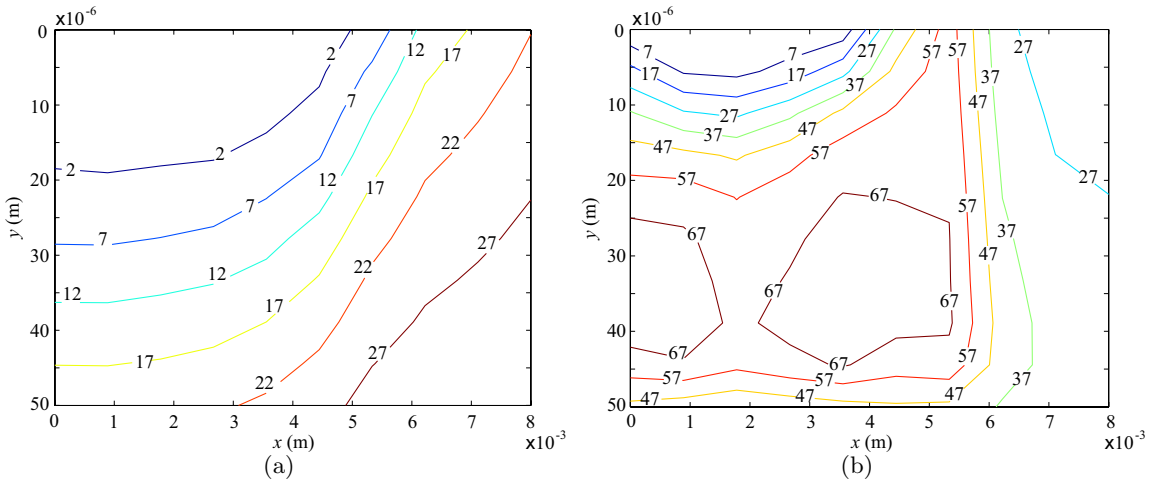

Figure 3. Isothermal lines in °C within epidermis at the end of (a) 60 ms cryogen spurt and (b) 0.45 ms laser pulse.

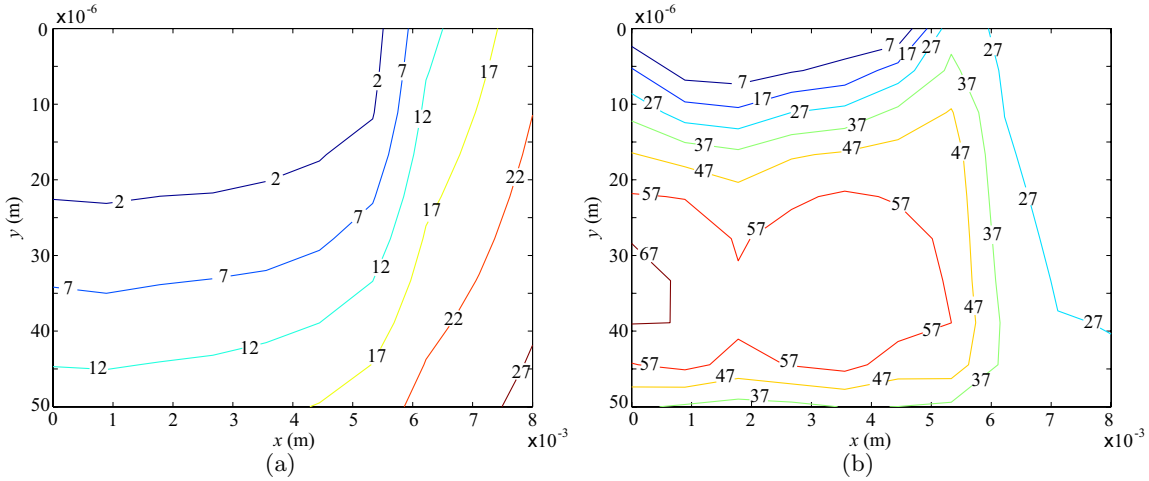

Figure 4. Isothermal lines in °C within epidermis at the end of (a) 60 ms cryogen spurt and a 60 ms delay, and (b) 0.45 ms laser pulse.

Isothermal contours within epidermis are shown in Fig. 4 for two different times during the second CSC-DLS sequence: at the end of the 60 ms cryogen spurt and a 60 ms delay, Fig. 4(a), and after a 0.45 ms laser pulse, Fig. 4(b). At the laser onset in Fig. 4(a): the lowest isothermal contour is still 2 °C but with a lateral range and depth of ≈ 5.5 mm and 23 μm, respectively; the highest isothermal contour is still 27 °C, however, the size of the epidermal region underneath the sprayed surface that has not been cooled at all has significantly reduced. Note also that separation between isothermal lines—respect to separations in the first CSC-DLS sequence—has increased showing a relative more uniform temperature field. Figure 4(b) shows that after laser irradiation, the epidermal regions within the 67 °C isothermal contours almost disappeared, the remaining region is located approximately at a 30–40 μm depth within a 0.5 mm radius; for a point at $x = 0$ and $y = 35$ μm, $\Omega_e = 0.2$. Similar thermal damage values are achieved at other points within this region. Therefore, enough epidermal protection is provided by this second CSC-DLS sequence, that is, the first sequence becomes feasible with the introduction of a time delay.

The temperature field within the blood vessels at the end of the laser pulse in the second CSC-DLS sequence

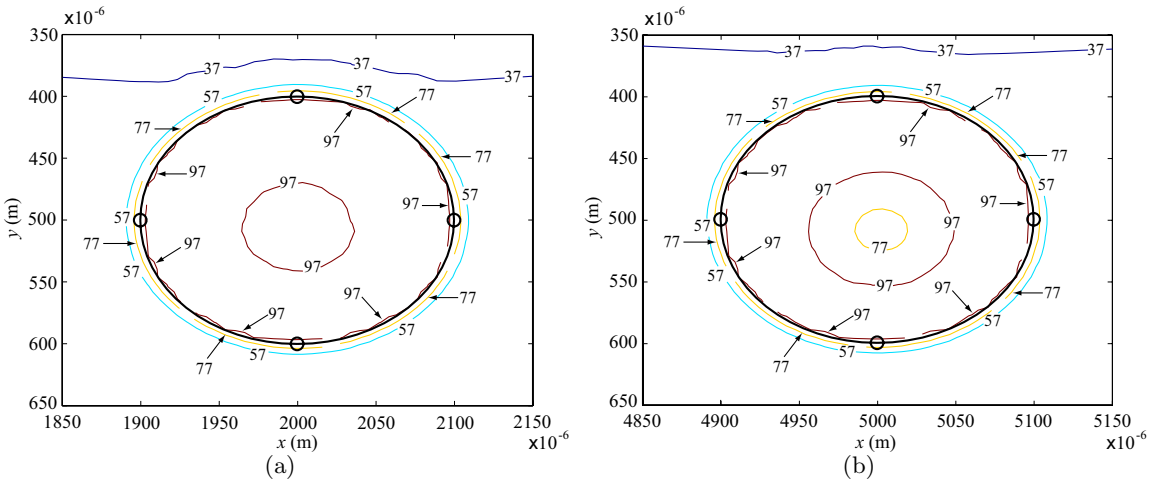

Figure 5. Isothermal lines in °C within dermis and (a) first and (b) second blood vessels at $t = 120.45 \times 10^{-3}$ s; –⊖– vessel wall.

is shown in Fig. 5. The blood vessel closer to the laser beam axis is shown in Fig. 5(a). Following a vertical line by the vessel center from top of the figure to the center of the vessel, we see isothermal contours at 37, 57, 77, 97 and 97 °C. This temperature sequence shows that T_b increases radially from the perimeter to certain inner radius and, subsequently, decreases from this inner radius to the center—this temperature changes are more evident in the second vessel, Fig. 5(b). The fact that there is a relative horizontal isotherm at 37 °C in both figures shows that precooling is still selective since the 60 ms delay does not affect the initial temperature of the blood vessels. As expected, the thermal profiles of the blood vessels are similar to each other since light deposition is uniform laterally. At the center of the inner and outermost vessel $\Omega_{b,1} = 3$ and $\Omega_{b,2} = 1.3$, respectively. The temperature field of the blood vessels at the end of laser exposure without using a delay (first sequence) is similar to that of Fig. 5 but not shown because of the excessive epidermal damage.

5. CONCLUSIONS

Epidermal protection provided by CSC is non-homogenous due to the inherent temporal and spatial complexity of sprays and the thermal-insulation nature of epidermis. As a consequence, there are significant temperature differences within the epidermis at the end of the cryogen spurt, which may result in thermal damage during laser exposure. A time delay between the end of the spurt and laser onset allows for a more homogenous temperature distribution in the epidermis reducing the risk of thermal damage. Because of the cooling selectivity of CSC, the initial temperature of the blood vessels embedded in the skin-cross section modeled herein was not affected by the delay. Temporal and lateral variations in surface heat transfer must be taken into account and, ideally, controlled to guarantee that sufficient epidermal protection is provided during CSC-assisted DLS. Thermal and optical numerical models of spray cooling and laser irradiation procedures that incorporate all the complexity of the problem are an essential research tool.

6. ACKNOWLEDGMENTS

This work was supported in part by the National Institute of Health (HD42057 to GA and AR47551 to JSN).

REFERENCES

1. J. S. Nelson, T. E. Milner, B. Anvari, B. S. Tanenbaum, S. Kimel, L. O. Svaasand, and S. L. Jacques, "Dynamic epidermal cooling during pulsed-laser treatment of port-wine stain - a new methodology with preliminary clinical evaluation," *Arch. Dermatol.* **131**(6), pp. 695–700, 1995.

2. J. S. Nelson, B. Majaron, and K. M. Kelly, "Active skin cooling in conjunction with laser dermatologic surgery," *Semin. Cutan. Med. Surg.* **19**(4), pp. 253–266, 2000.
3. W. Franco, G. X. Wang, J. S. Nelson, and G. Aguilar, "Radial heat transfer dynamics during cryogen spray cooling," in *Proc. ASME International Mechanical Engineering Congress & Exposition*, IMECE2004-59609, 2004.
4. B. Choi and A. J. Welch, "Infrared imaging of 2-D temperature distribution during cryogen spray cooling," *J. Biomech. Eng.-T ASME* **124**(6), pp. 669–675, 2002.
5. W. Franco, G. X. Wang, E. Karapetian, J. S. Nelson, and G. Aguilar, "Effect of surface thermal variations during cryogen spray cooling in dermatologic laser therapy," in *Proc. ILASS Americas*, 2004. 17th Annual Conference on Liquid Atomization and Spray Systems.
6. W. Star, "Diffusion theory of light transport," in *Optical-thermal Response of laser-irradiated Tissue*, A. J. Welch and M. J. C. van Gemert, eds., Plenum Publishing Corporation, New York, 1995.
7. S. J. Madsen, B. C. Wilson, M. S. Patterson, Y. D. Park, S. L. Jacques, and Y. Hefetz, "Experimental tests of a simple diffusion-model for the estimation of scattering and absorption-coefficients of turbid media from time-resolved diffuse reflectance measurements," *Applied Optics.* **31**(18), pp. 3509–3517, 1992.
8. M. S. Patterson, B. Chance, and B. C. Wilson, "Time resolved reflectance and transmittance for the non-invasive measurement of tissue optical-properties," *Applied Optics* **28**(12), pp. 2331–2336, 1989.
9. G. Shafirstein, W. Baumler, M. Lapidoth, S. F. P. E. North, and M. Waner, "A new mathematical approach to the diffusion approximation theory for selective photothermolysis modeling and its implication in laser treatment of port-wine stains," *Lasers Surg. Med.* **34**(4), pp. 335–347, 2004.
10. G. Aguilar, S. H. Diaz, E. J. Lavernia, and J. S. Nelson, "Cryogen spray cooling efficiency: Improvement of port wine stain laser therapy through muttiple-intermittent," *Lasers Surg. Med.* **31**(7), pp. 27–35, 2002.
11. W. Franco, G. X. Wang, J. S. Nelson, and G. Aguilar, "Radial and temporal variations in surface heat transfer during cryogen spray cooling," to appear in *Phys. Medicine Biology.*
12. J. P. Holman, *Heat Transfer*, McGraw Hill, New York, 1981.
13. Y. Rabin, "The effect of temperature-dependent thermal conductivity in heat transfer simulations of frozen biomaterials," *Cryoletters* **21**(3), pp. 163–170, 2000.
14. J. W. Valvano, J. R. Cochran, and K. R. Diller, "Thermal-conductivity and diffusivity of biomaterials measured with self-heated thermistors," *Int. J. Thermophys.* **6**(3), pp. 301–311, 1985.
15. F. A. Duck, *Physical properties of tissue*, Academic press, London, 1990.
16. A. Singh and P. L. Blackshear in *7th Int. Conf. on Medicine and Biological Engineering*, B. Jacobsen, ed.
17. F. C. Henriques, "Studies in thermal injury v. the predictability and significance of thermally induced rate processes leading to irreversible epidermal injury," *Arch. Pathol.* **43**, pp. 489–502, 1947.
18. J. R. Lepock, H. E. Frey, H. Bayne, and J. Markus, "Relationship of hyperthermia-induced hemolysis of human-erythrocytes to the thermal-denaturation of membrane-proteins," *Biochimica et Biophysica Acta* **2**, pp. 191–201, 1989.
19. J. Pearce and S. Thomsen, "Rate process analysis of thermal damage," in *Optical-thermal Response of laser-irradiated Tissue*, A. J. Welch and M. J. C. van Gemert, eds., Plenum Publishing Corporation, New York, 1995.
20. M. J. C. van Gemert, A. J. Welch, J. W. Pickering, and T. T. Oon, "Laser treatment of port wine stains," in *Optical-thermal Response of laser-irradiated Tissue*, A. J. Welch and M. J. C. van Gemert, eds., Plenum Publishing Corporation, New York, 1995.
21. J. V. Beck, B. Blackwell, and C. R. St. Clair, Jr., *Inverse heat conduction: ill posed problems*, Wiley, New York, 1985.